Journal of Oceanology and Limnology
Vol. 36 No. 3, P. 783-794, 2018
https://doi.org/10.1007/s00343-018-7072-2

Characterization of dominant giant rod-shaped magnetotactic bacteria from a low tide zone of the China Sea*

TENG Zhaojie (滕兆洁)[1, 2, 3], ZHANG Wenyan (张文燕)[1, 3, **], CHEN Yiran (陈一然)[1, 3], PAN Hongmiao (潘红苗)[1, 3], XIAO Tian (肖天)[1, 3], WU Long-Fei (吴龙飞)[4, 5]

[1] *CAS Key Laboratory of Marine Ecology & Environmental Sciences, Institute of Oceanology, Chinese Academy of Sciences, Qingdao 266071, China*

[2] *University of Chinese Academy of Sciences, Beijing 100049, China*

[3] *Laboratory of Marine Ecology and Environmental Science, Qingdao National Laboratory for Marine Science and Technology, Qingdao 266000, China*

[4] *Laboratoire de Chimie Bactérienne, UMR7283, Institut de Microbiologie de la Méditerranée, Aix-Marseille Université, CNRS, Marseille, France*

[5] *Laboratoire International Associé de la Bio-Minéralisation et Nano-Structures, CNRS, Marseille, France*

Received Mar. 7, 2017; accepted in principle Mar. 18, 2017; accepted for publication Mar. 31, 2017

Abstract Magnetotactic bacteria are a group of Gram-negative bacteria that synthesize magnetic crystals, enabling them to navigate in relation to magnetic field lines. Morphologies of magnetotactic bacteria include spirillum, coccoid, rod, vibrio, and multicellular morphotypes. The coccid shape is generally the most abundant morphotype among magnetotactic bacteria. Here we describe a species of giant rod-shaped magnetotactic bacteria (designated QR-1) collected from sediment in the low tide zone of Huiquan Bay (Yellow Sea, China). This morphotype accounted for 90% of the magnetotactic bacteria collected, and the only taxonomic group which was detected in the sampling site. Microscopy analysis revealed that QR-1 cells averaged (6.71±1.03)×(1.54±0.20) μm in size, and contained in each cell 42–146 magnetosomes that are arranged in a bundle formed one to four chains along the long axis of the cell. The QR-1 cells displayed axial magnetotaxis with an average velocity of 70±28 μm/s. Transmission electron microscopy based analysis showed that QR-1 cells had two tufts of flagella at each end. Phylogenetic analysis of the 16S rRNA genes revealed that QR-1 together with three other rod-shaped uncultivated magnetotactic bacteria are clustered into a deep branch of *Alphaproteobacteria*.

Keyword: *Alphaproteobacteria*; flagella; motility; rod-shaped magnetotactic bacteria

1 INTRODUCTION

Magnetotactic bacteria (MTB) are a heterogeneous group of fastidious microorganisms that are capable of biosynthesizing nano-sized, membrane-bound, magnetic iron-rich mineral particles termed magnetosomes (Lefèvre and Wu, 2013). The magnetosomes enable MTB to orient and navigate along geomagnetic field lines in a unique form of movement referred to as magnetotaxis. Magnetotaxis is thought to enable MTB to more rapidly locate optimal conditions in vertical chemical and/or redox gradients (Frankel et al., 1997; Schüler, 1999; Bazylinski and Frankel, 2004; Faivre and Schüler, 2008). MTB are ubiquitous in sediments of freshwater, brackish, marine, and hypersaline environments, and in the overlying chemically stratified water columns. Morphological and phylogenetic characterization of MTB has shown that this group is highly diverse (Lefèvre and Bazylinski, 2013).

MTB morphologies include spirillum, coccoid, rod, vibrio, and multicellular morphotypes (Bazylinski and Frankel, 2004). The magnetotactic cocci are the

* Supported by the National Natural Science Foundation of China (Nos. 41330962, 41276170) and the National Natural Science Foundation of China—Shandong Joint Fund for Marine Science Research Centers (No. U1606404)
** Corresponding author: zhangwy@qdio.ac.cn

most abundant morphotype of MTB and globally distributed in freshwater and marine sediments (Mann et al., 1990; Spring et al., 1992, 1995, 1998; Flies et al., 2005; Pan et al., 2008; Xing et al., 2008; Lin and Pan, 2009; Lin et al., 2009; Zhang et al., 2010, 2013; Bazylinski et al., 2013; Le Sage et al., 2013). Most MTB belong to the *Proteobacteria* phylum, including the *Alphaproteobacteria*, *Deltaproteobacteria* and *Gammaproteobacteria* classes; others belong to the *Nitrospira*, *Omnitrophica*, and *Candidatus* Latescibacteria phyla (Lefèvre et al., 2010, 2012; Kolinko et al., 2012; Williams et al., 2012; Lin and Pan, 2015). MTB belonging to the *Alphaproteobacteria* class represent the dominant proportion of uncultured MTB in many freshwater and marine environments (Spring et al., 1992, 1995, 1998; DeLong et al., 1993; Flies et al., 2005). Recently, it has been reported that the genomes of *Candidatus* Magnetococcus massalia MO-1 and *Magnetococcus marinus* MC-1 have coding sequences (CDSs) with a similarly high proportion of origins from *Alphaproteobacteria*, *Betaproteobacteria*, *Deltaproteobacteria* and *Gammaproteobacteria*, and represent a novel group of *Etaproteobacteria* (Ji et al., 2017).

Rod-shaped MTB have been affiliated with the *Alphaproteobacteria*, *Deltaproteobacteria* and *Gammaproteobacteria* classes and the Nitrospira phylum. The cultured rod-shaped strains SS-2 and BW-1, which belong to the *Deltaproteobacteria* (Lefèvre et al., 2011), share similar morphological characteristics with strains BW-2 and SS-5, which belong to the *Gammaproteobacteria* (Lefèvre et al., 2012). The rod-shaped MTB *Magnetobacterium bavaricum* (Spring et al., 1993), strain MHB-1 (Flies et al., 2005), and a rod-shaped MTB strain belonging to the '*C. Magnetobacterium*' genus (Lin et al., 2014) (affiliated with the Nitrospira phylum) contain multiple bullet-shaped magnetosome chains in their cells. Three other uncultured rod-shaped strains, clone 1-2-1 (named after its OTU), Cux-03, and CS-05, were proposed to be affiliated with the *Alphaproteobacteria*. The uncultured rod-shaped magnetotactic bacterium clone 1-2-1 was reported from the intertidal zone in Qingdao, China (Zhang et al., 2013), and two other uncultured rod-shaped strains Cux-03 and CS-05 have been reported from a marine intertidal mudflat sediment of the Wadden Sea (southeastern North Sea) and a freshwater sediment from Lake Chiemsee (Germany), respectively (Kolinko et al., 2013). It is notable that these three strains share an intriguing morphologically similarity. They are unusually large in size, are divided in two parts, have several refractive vesicles at the middle of the cell (visible by differential interference contrast microscopy), and all have elongated prismatic magnetosome crystals; both Cux-03 and CS-05 also have large electron dense inclusion particles at their poles.

In an intertidal zone in China we found a novel dominant giant rod-shaped MTB (designated strain QR-1: Qingdao Rod-shaped strain-1) that has a similar morphology to the three *Alphaproteobacteria* strains described above. In this study we used micromanipulation sorting combined with single cell whole genome amplification and fluorescence in situ hybridization (FISH) to identify the 16S rRNA gene of QR-1 and analyze its taxonomic affiliation.

2 MATERIAL AND METHOD

2.1 Site description

From 21 March to 7 July 2014, sediment samples were collected at low tide from a seawater pond located in the intertidal zone at Huiquan Bay (36°02′N, 120°20′E; Qingdao, China). Samples were collected approximately once each week (no sampling occurred in May) on a total of nine occasions. The pond had previously been used for the culture of sea cucumbers, but had not been used for this purpose for at least for 6 years prior to the collection of samples for this study. The pond comprises a permanently submerged part and a low tide area (Pan et al., 2008); during rising tides the pond forms a lagoon as water flows in from Huiquan Bay via the low tide area. The sampling site was immediately in front of the low tide area in the middle of the permanently submerged part. During the sampling period the salinity was approximately 31, and the pH of samples ranged from 7.78 to 8.12. The temperature during the sampling period ranged from 16 to 18°C. The salinity was determined using a hand-held refractometer (YW100; Chenhua, Chengdu, China), and the temperature and pH were measured using a benchtop pH/temperature meter (JENCO 6173, Shanghai, China).

2.2 Sampling and magnet collection of MTB

Surface sediments and overlying seawater (1:1 ratio) from the permanently submerged part of the pond were collected in 500 mL plastic bottles. Back to the laboratory, some samples were processed immediately, while others were stored under dim light at ambient temperature (approximately 25°C) for

subsequent analysis. Collection of MTB was performed as described previously (Moench and Konetzka, 1978). Cells were enriched by attaching the south poles of permanent magnets to the outside on two opposite sides of each plastic sampling bottle, adjacent to the water/sediment interface. After 30 min, approximately 1 mL of sample water was withdrawn using a Pasteur pipette from adjacent to the magnets and transferred to 1.5 mL centrifuge tubes for subsequent optical microscopy and micromanipulation sorting.

2.3 Optical and electron microscopy

The swimming behavior and cell morphology of the numerically dominant QR-1 strain were investigated on-site using differential interference contrast (DIC) microscopy (Olympus BX51 equipped with a DP71 camera system; Olympus, Tokyo, Japan) of cells enriched in a magnetic field applied to hanging drop preparations of the bacterium (Schüler, 2002). For transmission electron microscopy (TEM), cells collected by microsorting were adsorbed onto 200 mesh carbon-coated copper grids (Beijing Zhong Jing Ke Yi Technology Co., Ltd.) and examined (Hitachi H8100 TEM) without staining. The arrangement and morphology of the magnetosomes and the morphology of inclusions were assessed at 100 kV. The composition of magnetosomes and inclusions was investigated using energy-dispersive X-ray spectroscopy (EDXS) and high-resolution TEM (HRTEM; Jeol, JEM2100). To determine the surface morphology, cells were examined using scanning electron microscopy (SEM; KYKY-2800B, Beijing, China,) at 25 kV.

2.4 Microsorting and whole genome amplification

The procedures for microsorting and whole genome amplification (WGA) of the cells of strain QR-1 have been described previously (Chen et al., 2015). To phylogenetically identify the strains in this study, we combined microsorting with WGA, followed by polymerase chain reaction (PCR) analysis of the 16S rRNA genes.

2.5 Sequence analysis of 16S rRNA gene

The 16S rRNA gene was amplified from WGA products of the rod-shaped MTB. PCR using the bacteria-specific primers 27f and 1492r (Sangon Biotech, Shanghai, China) was performed using a Mastercycler (Eppendorf, German). The resulting PCR products were cloned into the pMD18-T vector (TaKaRa, Dalian, China) and transformed into competent *Escherichia coli* TOP10 cells. The clones were randomly selected for sequencing, which was carried out by Nanjing Genscript Biotechnology (Nanjing, China). The 16S rRNA gene sequences obtained were analyzed using the BLAST search program (http://www.ncbi.nlm.nih.gov/BLAST/). The 16S rRNA gene sequences of other strains were obtained from GenBank data; all of the 16S rRNA gene sequences were aligned using CLUSTAL W multiple alignment software; sequence identities were calculated using the BIOEDIT software.

A phylogenetic tree was constructed via the neighbor-joining method using MEGA 6, and bootstrap values were calculated from 1 000 replicates.

The 16S rRNA gene sequence has been submitted to the GenBank database under accession number KY317945.

2.6 Probe design

The 16S rRNA gene sequences of QR-1 were aligned with those of Cux-03, CS-05, and clone 1-2-1, and completely conserved regions were used to check for specificity by screening the bacterial DNA and structural RNA database sections of the GenBank database.

A specific probe QR197 (position 197–215; 5′-GAC GCA GGA CCC TCT CAA G-3′) was designed. The general probe EUB338 (5′-GCT GCC TCC CGT AGG AGT-3′), which anneals to the 16S rRNA genes of most bacteria, was also used as a control in specificity and permeability tests (Amann et al., 1990). The specific oligonucleotide DNA probes were labeled at the 5′ end with Cy5 dye, and the general probe was labeled at the 5′ end with 6-FAM (FITC). All probes were synthesized at Shanghai Sangon Biotech.

2.7 Fluorescence in situ hybridization

The tiptube-purified samples collected from the sampling site were fixed with 4% paraformaldehyde in artificial seawater (pH 7.2) for 12 h at 4°C, and then washed in artificial seawater. Other bacteria in the sample were used as positive controls for general probes, and as negative controls for specific probes. For each fixed sample, a 4-μL drop was placed onto an adhesion microscopy slide and dried for approximately 10 min at room temperature. The slide was then immersed in 50%, 80% and 100% ethanol for 3 min each, and then air-dried until the ethanol had evaporated. Hybridization buffer (13.5 μL) and 1.5 μL each of specific and general probe (50 ng/μL) were dropped onto the sample and incubated for 3 h at

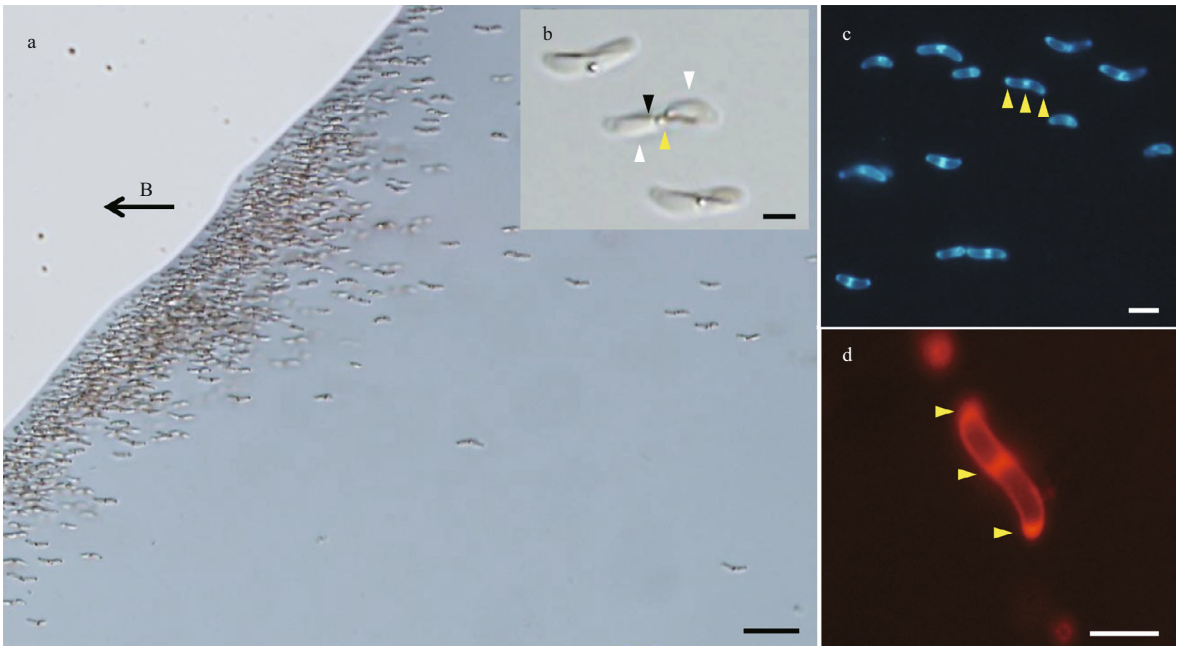

Fig.1 Optical microscopy morphology of the rod-shaped magnetotactic bacterium QR-1 from Huiquan Bay

a. differential interference contrast images of QR-1 showing that the strain is the dominant morphotype among the collected MTB; b. detailed morphological characteristics of QR-1, The black arrow indicates the direction of the applied magnetic field lines. The black, white, and yellow triangles indicate magnetosome chains, inclusion bodies, and refractive vesicles, respectively; c. fluorescence image showing that the cells emit strong blue fluorescence when exposed to UV light (wavelength: 330–385 nm) without staining. The yellow arrows indicate blue fluorescence at the ends and the middle of the cell; d. cell stained with Nile red, show lipid granules evident under blue light (wavelength: 450–480 nm). The yellow arrows indicate orange fluorescence at the ends and the middle of the cell. Scale bars=20 μm in panel a, 2 μm in panel b, and 5 μm in panels c and d.

46°C. A subsequent wash was performed at 48°C for 25 min using elution buffer. The slide was washed three times in dd H_2O, then dried. Fluorescence quenching agent (5 μL; Solarbio) was dropped onto the sample, and the slide was examined using fluorescence microscopy. The hybridization buffer contained 35% formamide, 1 mol/L Tris-HCl (pH 8.0), 5 mol/L NaCl, dd H_2O, and 10% SDS; the elution buffer contained 0.5 mol/L EDTA, 1 mol/L Tris-HCl (pH 8.0), 5 mol/L NaCl, dd H_2O, and 10% SDS.

3 RESULT

3.1 Occurrence and morphology of the giant rod-shaped strain QR-1

Freshly collected MTB comprised various cell shapes, including coccoid, vibrio, spirilla, and dominant rod-shaped morphotype. On six of the nine sampling occasions the rod-shaped magnetotactic bacterium QR-1 accounted for >90% of the MTB at the sampling site, with cells abundances up to 10^4 ind./cm^3 in samples that had not been incubated under laboratory conditions. It is noteworthy that strain QR-1 was the only morphotype of MTB present on 50% of the sampling occasions (Fig.1a). The cells of strain QR-1 averaged (6.71±1.03)×(1.54±0.20) μm in size (n=226), which is larger than most of the rod-shaped MTB previously reported, except for clone 1-2-1 (Zhang et al., 2013). The DIC microscopy revealed that the QR-1 cells were usually separated into two parts. Each part contained one inclusion particle and several refractive vesicles at the middle of the cell (Fig.1b). These morphological characteristic are very similar to those of clone 1-2-1 (Zhang et al., 2013), and strains Cux-03 and CS-05 (Kolinko et al., 2013), which are affiliated to the *Alphaproteobacteria*.

Fluorescence microscopy observation of cells without staining revealed blue florescent spots in the middle and at the poles of the cell (Fig.1c). Nile red staining showed that these spots may be lipid granules (Fig.1d).

3.2 Magnetosomes and inclusion bodiesgiant rod-shaped

Magnetosomes are membrane-enveloped nano-crystals that impart a magnetic moment and enable geomagnetic navigation of MTB (Schüler, 2008). TEM-based observations revealed that the giant rod-shaped MTB strain QR-1 contained 42 to 146 magnetosomes (n=15) per cell, arranged in a bundle

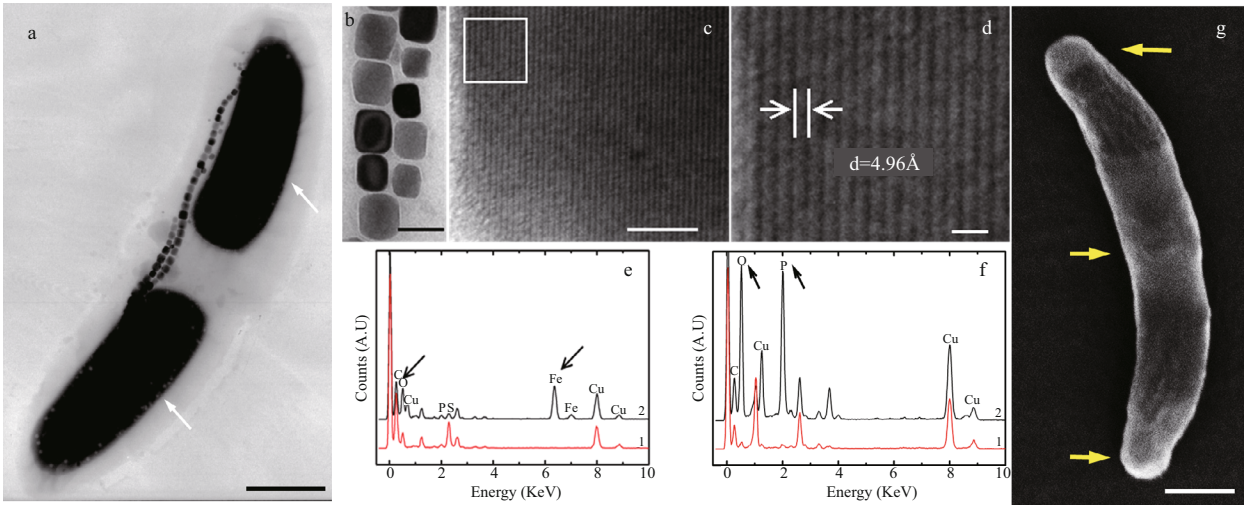

Fig.2 Ultrastructural analysis of QR-1

a. TEM images showing the characteristics of QR-1 cells; b. magnetosomes. The white arrows indicate the electron-dense inclusion bodies; c. HRTEM analysis of magnetite magnetosomes; d. a selected area at higher magnification; e. EDXS analysis of magnetite; f. polyphosphate. The black arrows identify peaks of iron and oxygen in panel e, and peaks of phosphorus and oxygen in panel f. g. SEM image showing the surface structure of QR-1 cells. The yellow arrows indicate the projecting imprint of lipid granules, coinciding with the morphological characteristics evident by TEM. Scale bars=1 μm in panels a and g, 50 nm in panel b, 5 nm in panel c, and 1 nm in panel d.

formed by 1–4 parallel chains along the long axis of the cell; approximately 53.3% of observed cells had two chains (Fig.2a). Each elongated prismatic magnetosome was 106±18 nm in length and 93±22 nm in width (n=271), and this produced a shape factor of approximately 0.876±0.1 (n=271) (Fig.2b). EDXS analysis indicated that the magnetosome crystals were composed of iron and oxygen, and analysis by HRTEM identified that the crystals were magnetite (Fig.2c, d, e). Multiple magnetosome chain bundles have previously been observed in strain clone 1-2-1 (Zhang et al., 2013), many *Nitrospira* strains from freshwater (Flies et al., 2005; Lin et al., 2012), and Multicellular Magnetotactic Prokaryotes (MMPs; Abreu et al., 2013; Zhou et al., 2013; Chen et al., 2015, 2016). EDXS analysis revealed that the two polar electron-dense structures contained large quantities of phosphorus and oxygen (Fig.2f), and were found to be composed of polyphosphate. SEM analysis of cellular morphology revealed a projecting imprint at the position of the lipid granules (Fig.2g), while TEM distinguished an electron-dense structure at each end of the cell (Fig.2a), as has been observed in Cux-03 and CS-05 (Kolinko et al., 2013). Each of the two elongated oval-shaped polyphosphate particles was approximately 2 μm long, and is much larger than similar structures in other strains (Silva et al., 2007; Lefèvre et al., 2009, 2012; Kolinko et al., 2013). Similar polyphosphate particles also occur in Cux-03 and CS-05 (Kolinko et al., 2013). Polyphosphate is a common type of inclusion body in bacteria, which use it as an energy source, phosphorus reserve material, or active metabolic regulator (Kulaev and Vagabov, 1983; Achbergerová and Nahálka, 2011). The use of polyphosphate by these MTB strains, and its possible role in regulation of magnetosome formation, is unclear.

3.3 Phylogenetic analysis

Identification of the taxonomic position of QR-1 in this study was performed by the micromanipulation sorting technique in combination with whole genome amplification and 16S rRNA gene amplification and sequencing, which has been shown to be a highly efficient method to identify MTB and MMPs in phylogenetic studies (Jogler et al., 2011; Kolinko et al., 2012, 2013; Zhang et al., 2014; Chen et al., 2015, 2016). Micromanipulation sorting enabled QR-1 with the giant rod morphotype to be separated from other bacteria (Chen et al., 2015) (see Materials and Methods). A total of 39 random clones were sequenced, and 27 of these (>69%) provided sequences most similar to Cux-03 (97% identity) (Schüler, 2002). All the 27 sequences belonged to the same OTU (QR-1), and among these 24 of the sequences differed by less than 0.4%. To verify the 16S rRNA gene sequence a specific oligonucleotide DNA probe was designed, based on the 16S rRNA gene sequence for QR-1. QR-1 cells were collected from the sampling site, along with other MTB as controls. The general probe recognized both the QR-1 and other marine bacteria, while the specific probe

only recognized QR-1 cells (Fig.3a, b). The three rod-shaped QR-1 cells were easy to tell apart by their shape based on fluorescence microscope, and the cells had strong fluorescence area in round shape may owing to high concentration of ribosomes and high ratios of hybridiztion (Frickmann et al., 2017). This result corroborates the authenticity of the 16S rRNA gene sequence belonging to QR-1 and shows the efficiency of micromanipulation-WGA-sequencing approach in taxonomic identification of MTB.

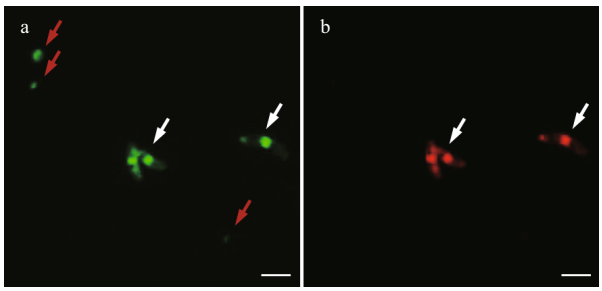

Fig.3 FISH analysis of QR-1

The same microscopic fields are shown following: a hybridization with the 5′-FAM labeled bacterial universal probe, EUB338; and b hybridization with the 5′-Cy5 labeled specific probe, QR197. White and red arrows indicate QR-1 cells and other MTB, respectively. Scale bars=5 μm.

Phylogenetic analysis of the 16S rRNA gene showed that QR-1 is closely related to three other rod-shaped MTB (Cux-03, CS-05, clone 1-2-1) (Fig.4). Although QR-1 showed a high level of identity (97%) with Cux-03 (Kolinko et al., 2013), the QR-1 cells are approximately double the size of Cux-03 (length: 6.7 μm versus 3.5 μm), and it has one to multiple magnetosome chains; this suggests that QR-1 may be a novel species. In addition, QR-1 has 92% identity with clone 1-2-1 (Zhang et al., 2013), and 89.4% identity with freshwater strain CS-05 (Kolinko et al., 2013). Other two uncultured clones MRT-120 (Xing et al., 2008) and QOCT164 which were also collected from Huiquan Bay and identified by mass collective method, clustered into the same clade with QR-1, suggesting that those two strains may be rod-shaped MTB. Interestingly, the uncultivated bacterium clone 1-2-1, Cux-03 and CS-05 were considered to be affiliated with *Alphaproteobacteria* because that is the most closely related Class (Kolinko et al., 2013; Zhang et al., 2013). However, these three strains together with QR-1 and most uncultivated magnetococcus bacterium were first clustered into a branch with *Cand*. Magnetococcus massalia MO-1

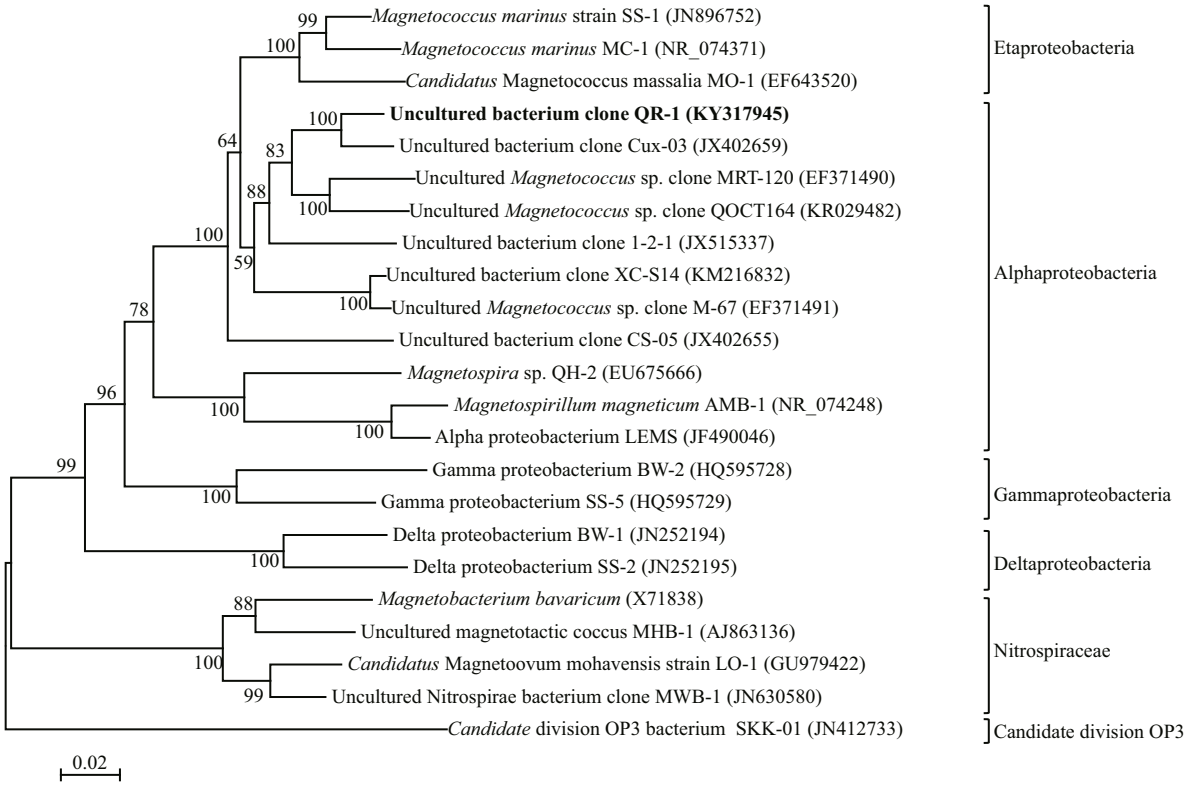

Fig.4 Phylogenetic tree of QR-1 and other MTB

The tree was constructed based on neighbor-joining analysis using full length 16S rRNA gene sequences, and the bootstrap values were calculated from 1 000 replicates. The sequence determined in this study is shown in bold. The GenBank accession numbers of the utilized sequences are indicated in parentheses. Rod-shaped MTB in the Alphaproteobacteria are circled in the dotted red box. Scale bar=0.02 substitutions per nucleotide position.

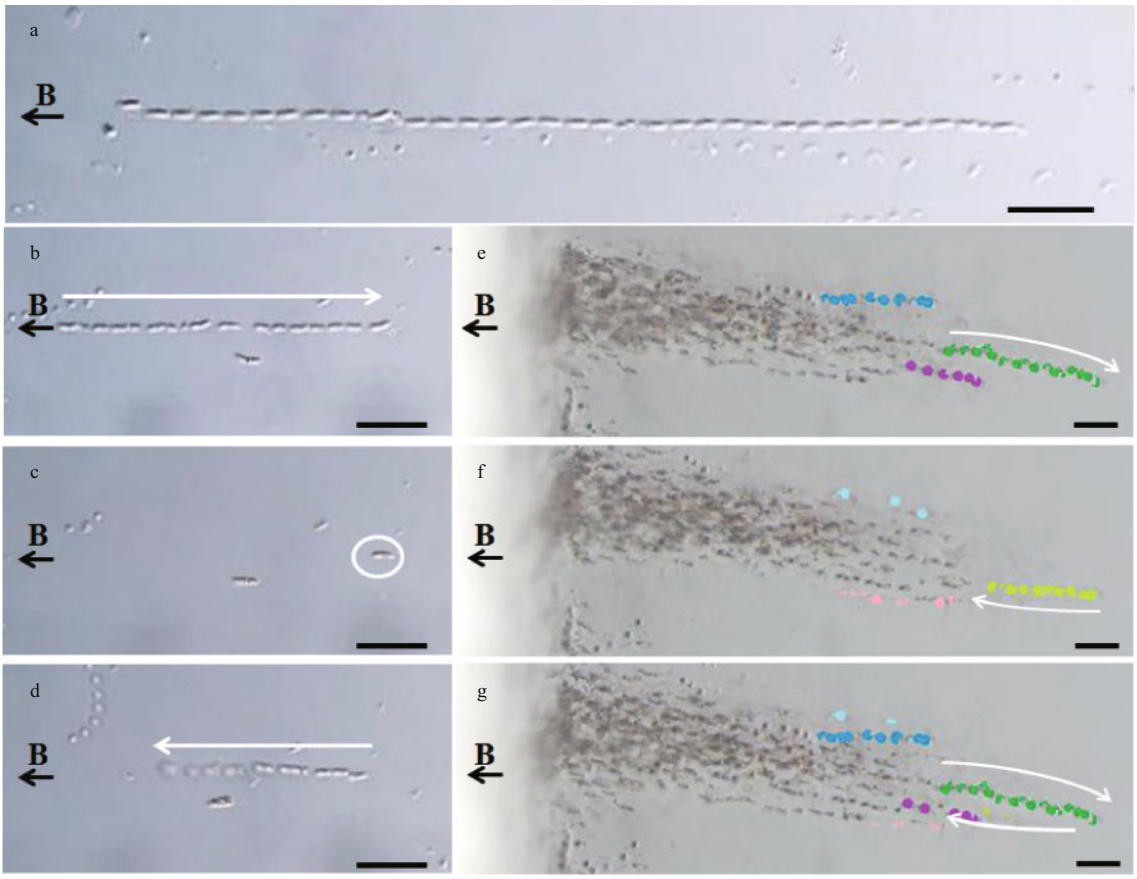

Fig.5 Motility of QR-1

a. composite images showing uniform velocity of QR-1; b. composite images showing excursion; c. transient cessation of motility; d. return swimming; e–g. composite images showing collective magneto-aerotaxis behavior of QR-1 cells. The black and white arrows indicate the direction of the applied magnetic field lines and the direction of movement of QR-1 cells, respectively. The white circle indicates non-moving cells. Scale bars=20 μm.

and *Magnetococcus marinus* MC-1 that are representatives of the novel *Etaproteobacteria* (Ji et al., 2017), and the branch clearly distinguish from representatives of magnetospillum and magnetovibrio. Alphaproteobacteria magnetotactic bacteria were cluttered with MO-1 and MC-1 that are representatives of the novel *Etaproteobacteria*, and genomic comparison is required to clarify the taxonomic classification of the QR-1 and its relatives.

3.4 Motility and flagella

For many bacteria, motility is essential for survival, growth, virulence, biofilm formation, and intra/interspecies interactions (Nan and Zusman, 2016). Motility associated with magnetotaxis typically involves the rotation of flagella, which are complex molecular machines that, like propellers, generate force to push cells forward or backward at differing speeds (Kearns, 2010).

The QR-1 cells swam at 20 to 132 μm/s (Fig.5a), with an average of 70±28 μm/s (n=85), which is slower than most ovoid-shaped MTB (Lefèvre et al., 2009, 2011; Zhang et al., 2012), but faster than that of the magnetotactic spirillum QH-2 (20–50 μm/s) (Zhu et al., 2010), *M. bavaricum* (average speed 40 μm/s) (Spring et al., 1993), and the slow moving MHB-1 (Flies et al., 2005). As with some magnetotactic spirilla including AMB-1, MS-1, and *Magnetospirillum magnetotacticum* (Balkwill et al., 1980; Spormann and Wolfe, 1984; Matsunaga et al., 1991), when exposed to an applied magnetic field QR-1 displayed axial magnetotaxis (Fig.5b, c, d), which involves cells being equally likely to swim parallel or antiparllel to the magnetic field, with random abrupt changes in direction (Faivre and Schüler, 2008). For these cells the magnetic field only represents an axis of swimming, but does not determine direction of movement (Frankel et al., 1997). When the direction of the applied magnetic field was reversed, QR-1 cells rotated 180°, but continued to swim back and forth; this response was similar to that of *M. magnetotacticum* (Frankel et al., 1997).

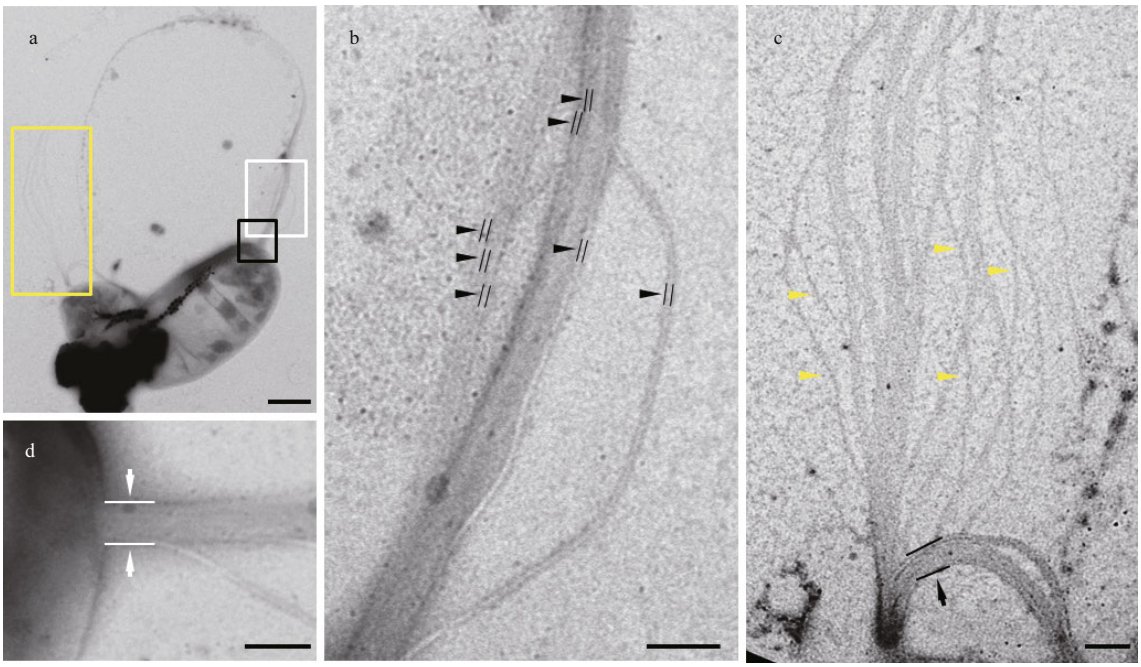

Fig.6 Flagella characteristics of QR-1

a. overall TEM image showing lophotrichous flagella; b. magnification of the area of the white rectangle in panel a, showing the flagella bundle at one end of the cell. The black arrows and parallel lines indicate 7 flagella in a bundle; c. magnification of the area of the yellow rectangle in panel a, showing the flagella bundle (black arrow and parallel lines) and numerous flagellar filaments (yellow arrows) at the other end of the cell; d. magnification of the black rectangle area in panel a, showing the root of the flagella bundle (indicated by white arrows and parallel lines). Scale bars=1 μm in panel a and 200 nm in panels b-d.

Bacteria have traditionally been viewed as unicellular organisms that grow as dispersed individual cells (Henrichsen, 1972). Remarkably, laboratory DIC microscopy observations of the edge of the hanging drop revealed a collective magneto-aerotaxis behavior by QR-1 cells apparently aggregating as multicellular groups rather than as individuals, when a magnetic field (500 Gs) was applied (Fig.5e, f, g). The composite image of the trajectories of groups of QR-1 cells revealed that this phenomenon was through the combined axial magnetotaxis of individual cells, which could be divided into 3 phases: (1) excursion swim from the droplet edge towards the center, at right angles to the magnetic field lines; (2) transient cessation of motility for approximately 0.2 s; and (3) return swimming back to the droplet edge parallel to the magnetic field lines.

TEM-based analysis showed that QR-1 cells have two tufts of flagella at each end of the cell (Fig.6a). Each tuft of flagella was composed of 7 flagellar filaments and many fibrils (Fig.6b, c). A similar flagella apparatus has been reported in the bilophotrichous flagella strains MC-1 (Frankel et al., 1997), MO-1 (Zhang et al., 2014), and QH-3 (Zhou et al., 2010). All the three coccid strains have flagellar sheaths, but no sheath was observed in QR-1. The diameters of the roots of the flagella bundles (Fig.6d), the filaments, and the fibrils was approximately 115 nm (n=21), 17.9±0.4 nm (n=123), and 12 nm (n=15), respectively.

4 DISCUSSION

In this study, a dominant rod-shaped MTB strain QR-1 was found from the seawater pond in intertidal zone. Compared with the low tide area, where the magnetotactic coccus QHL dominates (Pan et al., 2008), the permanently submerged part of the pond used as the sampling site in the present study was generally more stable and subject to less tidal disturbance. It had been reported that both environmental heterogeneity and geographic distance play significant roles in shaping the dominant populations in MTB communities (Lin et al., 2013). The geographic distributions of QR-1 and QHL are in very close proximity, suggesting that environmental heterogeneity between the ecological niches for these two bacteria may be the major factor determining the dominant species within the MTB communities at each site (Lin et al., 2013). At the population level, microbial growth followed established patterns known as the growth law (Schaechter et al., 1958). The individual cells' width did not change significantly between birth and division, and the average

instantaneous elongation rate was identical to the average nutrient-imposed growth rate of the population (Taheri-Araghi et al., 2015). Thus, the long rod-shaped QR-1 surpassed the nutrient-imposed growth rate of other MTB among MTB community, and then turned into the dominant population in biotope.

Our study shows that the giant rod-shaped QR-1 cells are larger than most of the rod-shaped MTB previously reported. So, how do QR-1 cells win in the competition for nutrients to maintain size homeostasis? Actually, bacteria are strictly osmotrophic, thus, their size is limited by surface area to volume (SA/V) ratios (Laflamme et al., 2009). Small cells, like bacteria, have large SA/V ratios. Typically, the larger SA/V is, the more efficiently the cell can exchange materials with the environment. The large SA/V precludes the need for complicated internal transport systems (Zhang, 2016). For bacteria, small variations in the width of individual cells had a strong negative effect on the SA/V values, whereas SA/V ratios are relatively constant when changing cell lengths (Steinberger et al., 2002; Laflamme et al., 2009). The QR-1 cells are longer than most of the MTB reported, but have no significant difference with them in width. Therefore, the SA/V rations of QR-1 cells are not significantly affected by cell widths, and their lengths influence the surface area and volume more significantly than the SA/V. Hence, other growth strategies to increase SA/V allowing for rapid and effective transport of nutrients directly through the integument into QR-1 cells are needed. *Thiomargarita* are largest bacteria with sizes up to 750 μm in diameter (Schulz and Schulz, 2005). However, the tremendous dimensions greatly reduce the feasibility osmotrophy which is restricted to bacteria with sizes 100 μm (Schulz and Jørgensen, 2001). To reduce the SA/V threshold, the *Thiomargarita* cell usually contain a large central vacuole and numerous sulfur particles which strategically reducing the overall active organic volume to increase SA/V. In fact, this growth strategy is also used by QR-1 cells because they possessed two large oval-shaped polyphosphate particles. The incorporation of inactive matter within the volume significantly restricts the effective volume used by the organism, thereby allowing QR-1 cells to maintain high SA/V ratios and also consistent with morphological expectations for osmotrophs.

Recently, microsorting and WGA are widely used as effective techniques for MTB strain isolation and identification (Jogler et al., 2011; Kolinko et al., 2012, 2013; Zhou et al., 2012; Chen et al., 2015, 2016). These techniques easily linked phylo- to morphotypes and led to the discovery of novel low-abundant MTB (Kolinko et al., 2013), and facilitated the amplification and de novo assembly of whole genomes even from an individual bacterial cell (Rodrigue et al., 2009; Woyke et al., 2010). Here, microsorting and WGA were applied for the phylogenetic and ultrastructural analysis of giant rod-shaped QR-1. This strain is phylogenetically affiliated closer with the marine strains clone 1-2-1 and Cux-03 than to the freshwater strain CS-05, indicating that phylotype is related to habitat conditions (Zhang et al., 2010). Despite their different geographic origins and ecology, these three marine strains share considerable morphological similarity, and clustered into one clade in the phylogenetic tree, apparently separate from other morphotypes; this indicates that these morphologically distinct strains may have originated from a common ancestor.

It should be noted that the flagella apparatus of QR-1 cells was first reported in rod-shaped MTB, which have mostly been reported to be monotrichous (Spring et al., 1993; Lefèvre et al., 2010, 2011; Kolinko et al., 2013). It has been reported that, during swimming motility, the flagella of a cell coalesce into a bundle and rotate to propel the bacterium forward, while tumbling can occur when only a single flagellum changes its direction of rotation (Kearns, 2010). The bundling of flagella effectively increases flagellar stiffness during rotation, and makes force generation more efficient in viscous liquids (Atsumi et al., 1996; Zhang et al., 2014). Because of this powerful flagella apparatus, strain QR-1 exhibited distinct magnetotactic motility and demonstrated higher speeds than other reported rod-shaped strains (Spring et al., 1993; Flies et al., 2005).

With the powerful flagella apparatus of QR-1, the cells group exhibited a special collective magneto-aerotaxis behavior which distinguished them from all rod-shaped MTB reported previously (Spring et al., 1993; Flies et al., 2005; Lefèvre et al., 2011; 2012; Kolinko et al., 2013). It was inferred that this behavior occurred in conjunction with aerotaxis, with cells exhibiting a positive response to the marked change in oxygen concentration ($[O_2]$) when they were transferred from sediment to the hanging drop (Mao and Liu, 2015). QR-1 cells probably have an oxygen sensory system (Taylor, 1983; Spormann and Wolfe, 1984) that can determine the change in $[O_2]$, enabling them to regulate the direction of flagellar rotation

(Wadhams and Armitage, 2004; Turner et al., 2010). One interpretation for the observed movement is that the accumulation of cells in high densities may result in depletion of oxygen (Frankel et al., 1997) to a concentration lower than optimum, resulting in clockwise flagellar rotation and swimming at right angles to the magnetic field until a higher [O_2] is encountered. At this point the cells pause and reverse flagellar direction to counterclockwise, then swim parallel to the magnetic field until they reach a low [O_2] threshold. Whether this behavior occurs in situ is unknown.

5 CONCLUSION

The giant rod-shaped MTB QR-1 described here were dominant morphotype in sampling environment, contrary to previous reports that magnetotactic cocci are the most abundant morphotype of MTB. The strain QR-1 was separated into two parts with one polyphosphate particle and several lipid granules at the middle of the cell. Each cell usually possessed 1–4 parallel magnetosome chains arranged along the long axis of the cell. These morphology characteristics were similar to those reported rod-shaped MTB belonged to *Alphaproteobacteria*. To identity the taxonomic position of QR-1, micromanipulation sorting technique in combination with WGA and FISH were performed, and the analysis showed that QR-1 affiliated within the deep branch of *Alphaproteobacteria*. Besides, the QR-1 cells swam faster than other rod-shaped MTB and displayed a unique collective magneto-aerotaxis behavior which was a combined axial magnetotaxis of individual cells. All of these motility characteristics were due to the powerful flagella apparatus. QR-1 cells have two tufts of flagella with 7 flagellar filaments and many fibrils in each tuft, and this kind of flagella apparatus was first reported in rod-shaped MTB.

6 DATA AVAILABILITY STATEMENT

Sequence data that support the findings of this study have been deposited in the GenBank database with accession number KY317945.

7 ACKNOWLEDGEMENT

We thank XU Jianhong for his assistance with biological sampling, JIANG Ming, LIU Jing, and MA Xicheng for their assistance with the TEM analysis, and LIU Wei for supporting our SEM observations.

References

Abreu F, Silva K T, Leão P, Guedes I A, Keim C N, Farina M, Lins U. 2013. Cell adhesion, multicellular morphology, and magnetosome distribution in the multicellular magnetotactic prokaryote *Candidatus* Magnetoglobus multicellularis. *Microsc. Microanal.*, **19**(3): 535-543.

Achbergerová L, Nahálka J. 2011. Polyphosphate-an ancient energy source and active metabolic regulator. *Microb. Cell. Fact.*, **10**(1): 63.

Amann R I, Krumholz L, Stahl D A. 1990. Fluorescent-oligonucleotide probing of whole cells for determinative, phylogenetic, and environmental studies in microbiology. *J. Bacteriol.*, **172**(2): 762-770.

Atsumi T, Maekawa Y, Yamada T, Kawagishi I, Imae Y, Homma M. 1996. Effect of viscosity on swimming by the lateral and polar flagella of Vibrio alginolyticus. *J. Bacteriol.*, **178**(16): 5 024-5 026.

Balkwill D L, Maratea D, Blakemore R P. 1980. Ultrastructure of a magnetotactic spirillum. *J. Bacteriol.*, **141**(3): 1 399-1 408.

Bazylinski D A, Frankel R B. 2004. Magnetosome formation in prokaryotes. *Nat. Rev. Microbiol.*, **2**(3): 217-230.

Bazylinski D A, Williams T J, Lefèvre C T, Berg R J, Zhang C L, Bowser S S, Dean A J, Beveridge T J. 2013. *Magnetococcus marinus* gen. nov., sp. nov., a marine, magnetotactic bacterium that represents a novel lineage (*Magnetococcaceae* fam. nov., *Magnetococcales* ord. nov.) at the base of the *Alphaproteobacteria*. *Int. J. Syst. Evol. Microbiol.*, **63**(3): 801-808.

Chen Y R, Zhang R, Du H J, Pan H M, Zhang W Y, Zhou K, Li J H, Xiao T, Wu L F. 2015. A novel species of ellipsoidal multicellular magnetotactic prokaryotes from Lake Yuehu in China. *Environ. Microbiol.*, **17**(3): 637-647.

Chen Y R, Zhang W Y, Zhou K, Pan H M, Du H J, Xu C, Xu J H, Pradel N, Santini C L, Li J H, Huang H, Pan Y X, Xiao T, Wu L F. 2016. Novel species and expanded distribution of ellipsoidal multicellular magnetotactic prokaryotes. *Environ. Microbiol. Rep.*, **8**(2): 218-226.

DeLong E F, Frankel R B, Bazylinski D A. 1993. Multiple evolutionary origins of magnetotaxis in bacteria. *Science*, **259**(5096): 803-806.

Faivre D, Schüler D. 2008. Magnetotactic bacteria and magnetosomes. *Chem. Rev.*, **108**(11): 4 875-4 898.

Flies C B, Peplies J, Schüler D. 2005. Combined approach for characterization of uncultivated magnetotactic bacteria from various aquatic environments. *Appl. Environ. Microbiol.*, **71**(5): 2 723-2 731.

Frankel R B, Bazylinski D A, Johnson M S, Taylor B L. 1997. Magneto-aerotaxis in marine coccoid bacteria. *Biophys. J.*, **73**(2): 994-1 000.

Frickmann H, Zautner A E, Moter A, Kikhney J, Hagen R M, Stender H, Poppert S. 2017. Fluorescence *in situ* hybridization (FISH) in the microbiological diagnostic routine laboratory: a review. *Crit. Rev. Microbiol.*, **43**(3): 263-293.

Henrichsen J. 1972. Bacterial surface translocation: a survey

and a classification. *Bacteriol*. *Rev*., **36**(4): 478-503.

Ji B Y, Zhang S D, Zhang W J, Rouy Z, Alberto F, Santini C L, Mangenot S, Gagnot S, Philippe N, Pradel N, Zhang L C, Tempel S, Li Y, Médigue C, Henrissat B, Coutinho P M, Barbe V, Talla E, Wu L F. 2017. The chimeric nature of the genomes of marine magnetotactic coccoid-ovoid bacteria defines a novel group of *Proteobacteria*. *Environ*. *Microbiol*., **19**(3): 1 103-1 119, https://doi.org/10.1111/1462-2920.13637.

Jogler C, Wanner G, Kolinko S, Niebler M, Amann R, Petersen N, Kube M, Reinhardt R, Schüler D. 2011. Conservation of proteobacterial magnetosome genes and structures in an uncultivated member of the deep-branching *Nitrospira* phylum. *Proc*. *Natl*. *Acad*. *Sci*. *USA*, **108**(3): 1 134-1 139.

Kearns D B. 2010. A field guide to bacterial swarming motility. *Nat*. *Rev*. *Microbiol*., **8**(9): 634-644.

Kolinko S, Jogler C, Katzmann E, Wanner G, Peplies J, Schüler D. 2012. Single-cell analysis reveals a novel uncultivated magnetotactic bacterium within the candidate division OP3. *Environ*. *Microbiol*., **14**(7): 1 709-1 721.

Kolinko S, Wanner G, Katzmann E, Kiemer F, Fuchs B M, Schüler D. 2013. Clone libraries and single cell genome amplification reveal extended diversity of uncultivated magnetotactic bacteria from marine and freshwater environments. *Environ*. *Microbiol*., **15**(5): 1 290-1 301.

Kulaev I S, Vagabov V M. 1983. Polyphosphate metabolism in micro-organisms. *Adv Microb Physiol*, **24**: 83-171.

Laflamme M, Xiao S H, Kowalewski M. 2009. Osmotrophy in modular Ediacara organisms. *Proc*. *Natl*. *Acad*. *Sci*. *USA*, **106**(34): 14 438-14 443.

Le Sage D, Arai K, Glenn D R, DeVience S J, Pham L M, Rahn-Lee L, Lukin M D, Yacoby A, Komeili A, Walsworth R L. 2013. Optical magnetic imaging of living cells. *Nature*, **496**(7446): 486-489.

Lefèvre C T, Abreu F, Schmidt M L, Lins U, Frankel R B, Hedlund B P, Bazylinski D A. 2010. Moderately thermophilic magnetotactic bacteria from hot springs in Nevada. *Appl*. *Environ*. *Microbiol*., **76**(11): 3 740-3 743.

Lefèvre C T, Bazylinski D A. 2013. Ecology, diversity, and evolution of magnetotactic bacteria. *Microbiol*. *Mol*. *Biol*. *Rev*., **77**(3): 497-526.

Lefèvre C T, Bernadac A, Kui Y Z, Pradel N, Wu L F. 2009. Isolation and characterization of a magnetotactic bacterial culture from the Mediterranean Sea. *Environ*. *Microbiol*., **11**(7): 1 646-1 657.

Lefèvre C T, Frankel R B, Abreu F, Lins U, Bazylinski D A. 2011. Culture-independent characterization of a novel, uncultivated magnetotactic member of the *Nitrospirae* phylum. *Environ*. *Microbiol*., **13**(2): 538-549.

Lefèvre C T, Schmidt M L, Viloria N, Trubitsyn D, Schüler D, Bazylinski D A. 2012. Insight into the evolution of magnetotaxis in *Magnetospirillum* spp., based on mam gene phylogeny. *Appl*. *Environ*. *Microbiol*., **78**(20): 7 238-7 248.

Lefèvre C T, Wu L F. 2013. Evolution of the bacterial organelle responsible for magnetotaxis. *Trends Microbiol*., **21**(10): 534-543.

Lin W, Bazylinski D A, Xiao T, Wu L F, Pan Y X. 2014. Life with compass: diversity and biogeography of magnetotactic bacteria. *Environ*. *Microbiol*., **16**(9): 2 646-2 658.

Lin W, Li J H, Pan Y X. 2012. Newly isolated but uncultivated magnetotactic bacterium of the phylum *Nitrospirae* from Beijing, China. *Appl*. *Environ*. *Microbiol*., **78**(3): 668-675.

Lin W, Li J H, Schüler D, Jogler C, Pan Y X. 2009. Diversity analysis of magnetotactic bacteria in Lake Miyun, northern China, by restriction fragment length polymorphism. *Syst*. *Appl*. *Microbiol*., **32**(5): 342-350.

Lin W, Pan Y X. 2009. Uncultivated magnetotactic cocci from yuandadu park in beijing, China. *Appl*. *Environ*. *Microbiol*., **75**(12): 4 046-4 052.

Lin W, Pan Y X. 2015. A putative greigite-type magnetosome gene cluster from the candidate phylum *Latescibacteria*. *Environ*. *Microbiol*. *Rep*., **7**(2): 237-242.

Lin W, Wang Y Z, Gorby Y, Nealson K, Pan Y X. 2013. Integrating niche-based process and spatial process in biogeography of magnetotactic bacteria. *Sci*. *Rep*., **3**(1): 1643.

Mann S, Sparks N H C, Board R G. 1990. Magnetotactic bacteria: microbiology, biomineralization, palaeomagnetism and biotechnology. *Adv*. *Microb*. *Physiol*., **31**: 125-181.

Mao X, Liu X. 2015. An initial study of the influences of oxygen conditions on wild-type magnetotactic bacteria in sediment. *Chin*. *Sci*. *Bull*., **60**(1): 88-96. (in Chinese with English abstract)

Matsunaga T, Sakaguchi T, Tadokoro F. 1991. Magnetite formation by a magnetic bacterium capable of growing aerobically. *Appl*. *Microbiol*. *Biotechnol*., **35**(5): 651-655.

Moench T T, Konetzka W A. 1978. A novel method for the isolation and study of a magnetotactic bacterium. *Arch*. *Microbiol*., **119**(2): 203-212.

Nan B Y, Zusman D R. 2016. Novel mechanisms power bacterial gliding motility. *Mol*. *Microbiol*., **101**(2): 186-193.

Pan H M, Zhu K L, Song T, Yu-Zhang K, Lefèvre C, Xing S, Liu M, Zhao S J, Xiao T, Wu L F. 2008. Characterization of a homogeneous taxonomic group of marine magnetotactic cocci within a low tide zone in the China Sea. *Environ*. *Microbiol*., **10**(5): 1 158-1 164.

Rodrigue S, Malmstrom R R, Berlin A M, Birren B W, Henn M R, Chisholm S W. 2009. Whole genome amplification and *de novo* assembly of single bacterial cells. *PLoS One*, **4**(9): e6864.

Schaechter M, Maaløe O, Kjeldgaard N O. 1958. Dependency on medium and temperature of cell size and chemical composition during balanced growth of *Salmonella typhimurium*. *J*. *Gen*. *Microbiol*., **19**(3): 592-606.

Schüler D. 1999. Formation of magnetosomes in magnetotactic bacteria. *J*. *Mol*. *Microbiol*. *Biotechnol*., **1**(1): 79-86.

Schüler D. 2002. The biomineralization of magnetosomes in *Magnetospirillum gryphiswaldense*. *Int*. *Microbiol*., **5**(4): 209-214.

Schüler D. 2008. Genetics and cell biology of magnetosome formation in magnetotactic bacteria. *FEMS Microbiol*. *Rev*., **32**(4): 654-672.

Schulz H N, Jørgensen B B. 2001. Big bacteria. *Annu*. *Rev*. *Microbiol*., **55**(1): 105-137.

Schulz H N, Schulz H D. 2005. Large sulfur bacteria and the formation of phosphorite. *Science*, **307**(5708): 416-418.

Silva K T, Abreu F, Almeida F P, Keim C N, Farina M, Lins U. 2007. Flagellar apparatus of south-seeking many-celled magnetotactic prokaryotes. *Microsc*. *Res*. *Tech*., **70**(1): 10-17.

Spormann A M, Wolfe R S. 1984. Chemotactic, magnetotactic and tactile behaviour in a magnetic spirillum. *FEMS Microbiol*. *Lett*., **22**(3): 171-177.

Spring S, Amann R, Ludwig W, Schleifer K H, Petersen N. 1992. Phylogenetic diversity and identification of nonculturable magnetotactic bacteria. *Syst*. *Appl*. *Microbiol*., **15**(1): 116-122.

Spring S, Amann R, Ludwig W, Schleifer K H, Schüler D, Poralla K, Petersen N. 1995. Phylogenetic analysis of uncultured magnetotactic bacteria from the alpha-subclass of *Proteobacteria*. *Syst*. *Appl*. *Microbiol*., **17**(4): 501-508.

Spring S, Amann R, Ludwig W, Schleifer K H, van Gemerden H, Petersen N. 1993. Dominating role of an unusual magnetotactic bacterium in the microaerobic zone of a freshwater sediment. *Appl*. *Environ*. *Microbiol*., **59**(8): 2 397-2 403.

Spring S, Lins U, Amann R, Schleifer K H, Ferreira L C S, Esquivel D M S, Farina M. 1998. Phylogenetic affiliation and ultrastructure of uncultured magnetic bacteria with unusually large magnetosomes. *Arch*. *Microbiol*., **169**(2): 136-147.

Steinberger R E, Allen A R, Hansa H G, Holden P A. 2002. Elongation correlates with nutrient deprivation in pseudomonas aeruginosa-unsaturates biofilms. *Microb*. *Ecol*., **43**(4): 416-423.

Taheri-Araghi S, Bradde S, Sauls J T, Hill N S, Levin P A, Paulsson J, Vergassola M, Jun S. 2015. Cell-size control and homeostasis in bacteria. *Curr*. *Biol*., **25**(3): 385-391.

Taylor B L. 1983. How do bacteria find the optimal concentration of oxygen? *Trends Biochem*. *Sci*., **8**(12): 438-441.

Turner L, Zhang R J, Darnton N C, Berg H C. 2010. Visualization of flagella during bacterial swarming. *J*. *Bacteriol*., **192**(13): 3 259-3 267.

Wadhams G H, Armitage J P. 2004. Making sense of it all: bacterial chemotaxis. *Nat*. *Rev*. *Mol*. *Cell Biol*., **5**(12): 1 024-1 037.

Williams T J, Lefèvre C T, Zhao W D, Beveridge T J, Bazylinski D A. 2012. *Magnetospira thiophila* gen. nov., sp. nov., a marine magnetotactic bacterium that represents a novel lineage within the *Rhodospirillaceae* (*Alphaproteobacteria*). *Int*. *J*. *Syst*. *Evol*. *Microbiol*., **62**(10): 2 443-2 450.

Woyke T, Tighe D, Mavromatis K, Clum A, Copeland A, Schackwitz W, Lapidus A, Wu D Y, McCutcheon J P, McDonald B R, Moran N A, Bristow J, Cheng J F. 2010. One bacterial cell, one complete genome. *PLoS One*, **5**(4): e10314.

Xing S E, Pan H M, Zhu K L, Xiao T, Wu L F. 2008. Diversity of marine magnetotactic bacteria in the Huiquan bay near Qingdao city. *Chin*. *High Technol*. *Lett*., **18**(3): 312-317. (in Chinese with English abstract)

Zhang W J, Li Y, Wu L F. 2014. Complex composition and exquisite architecture of bacterial flagellar propellers. *Chin*. *Sci*. *Bull*., **59**(20): 1 912-1 918. (in Chinese with English abstract)

Zhang W Y, Zhang S D, Xiao T, Pan Y X, Wu L F. 2010. Geographical distribution of magnetotactic bacteria. *Environ*. *Sci*., **31**(2): 450-458. (in Chinese with English abstract)

Zhang W Y, Zhou K, Pan H M, Du H J, Chen Y R, Zhang R, Ye W N, Lu C J, Xiao T, Wu L F. 2013. Novel rod-shaped magnetotactic bacteria belonging to the class *Alphaproteobacteria*. *Appl*. *Environ*. *Microbiol*., **79**(9): 3 137-3 140.

Zhang W Y, Zhou K, Pan H M, Yue H D, Jiang M, Xiao T, Wu L F. 2012. Two genera of magnetococci with bean-like morphology from intertidal sediments of the Yellow Sea, China. *Appl*. *Environ*. *Microbiol*., **78**(16): 5 606-5 611.

Zhang X H. 2016. Marine Microbiology. 2nd edn. Science Press, Beijing, China. p.10-11. (in Chinese)

Zhou K, Pan H M, Yue H D, Xiao T, Wu LF. 2010. Architecture of flagellar apparatus of marine magnetotactic cocci from Qingdao. *Mar*. *Sci*., **34**(12): 88-92. (in Chinese with English abstract)

Zhou K, Zhang W Y, Pan H M, Li J H, Yue H D, Xiao T, Wu L F. 2013. Adaptation of spherical multicellular magnetotactic prokaryotes to the geochemically variable habitat of an intertidal zone. *Environ*. *Microbiol*., **15**(5): 1 595-1 605.

Zhou K, Zhang W Y, Yu-Zhang K, Pan H M, Zhang S D, Zhang W J, Yue H D, Li Y, Xiao T, Wu L F. 2012. A novel genus of multicellular magnetotactic prokaryotes from the Yellow Sea. *Environ*. *Microbiol*., **14**(2): 405-413.

Zhu K L, Pan H M, Li J H, Yu-Zhang K, Zhang S D, Zhang W Y, Zhou K, Yue H D, Pan Y X, Xiao T, Wu L F. 2010. Isolation and characterization of a marine magnetotactic spirillum axenic culture QH-2 from an intertidal zone of the China Sea. *Res*. *Microbiol*., **161**(4): 276-283.